Upgrading of ferruginous manganese tailings by hydrogen-rich reduction for the ferroalloy industry

by D.A. Barrett[1], M. Tadie[1], B. von der Heyden[1], R. Cromarty[2]

Affiliation:
[1]African Rainbow Minerals Chair in Geometallurgy, Stellenbosch University, South Africa
[2]University of Pretoria, South Africa

Correspondence to:
D.A. Barrett

Email:
19barrda@gmail.com

Dates:
Received: 19 May. 2026
Published: July. 2026

How to cite:
Barrett D.A., Tadie M. von der Heyden B. Cromarty R. 2026. Upgrading of ferruginous manganese tailings by hydrogen-rich reduction for the ferroalloy industry. *Journal of the Southern African Institute of Mining and Metallurgy*, vol. 126, no. 7, pp. – 385 - 394

DOI ID:
https://doi.org/10.17159/2411-9717/1007/2026

ORCiD:
D.A. Barrett
https://orcid.org/0009-0006-4390-0502
M. Tadie
https://orcid.org/0000-0003-3111-5188
B. von der Heyden,
https://orcid.org/0000-0002-4006-9278
R Cromarty
https://orcid.org/0000-0002-2424-040X

This paper is based on a presentation given at the SAIMM Pyrometallurgy International Conference 2026, 26-28 May 2026, CSIR International Convention Centre, Pretoria, South Africa

Abstract

This paper investigated the prereduction of ferruginous manganese tailings from the Nchwaning mine by isothermal reduction between 650 °C and 1050 °C. The treated tailings underwent subsequent magnetic separation to upgrade the Mn/Fe ratio and manganese grade so that the tailings can be used as high-quality ferroalloy feedstock. The tailings contain recoverable manganese but is penalised by elevated and complex iron content. There is a high degree of mineralogical variability found in the untreated tailings. Iron is present both as hematite and in solid solution within manganese minerals such as bixbyite, braunite, and braunite II. A hydrogen atmosphere was used in this paper as it is sufficiently reducing to produce metallic iron that can be separated magnetically. Lime and silica additives were investigated to determine their influence on Fe reduction kinetics and globule formation, which impacts the separability of Fe and Mn. Optical microscopy and SEM analysis of the treated material revealed distinct metallurgical behaviour between iron reduced from hematite – forming larger globules (50 µm to 600 µm) – and iron reduced from Mn-hosted phases, which formed smaller globules (0.1 µm to 2 µm). Relatively milder reducing conditions achieved the highest Mn/Fe ratio of 4.52 and an Mn grade of 57 wt.%. While below the desired target specification (Mn/Fe of at least 7.5 wt.% and Mn grade of at least 44 wt.%), this can still be met by blending the product stream with other low-grade Mn ores that contain minimal Fe. These findings highlight the potential for the upgradation of ferruginous manganese tailings.

Keywords

gravity concentration, trough length, heavy mineral sands, recovery

Introduction

Manganese is a mineral of global economic importance due to its contributions to the steel industry, where it is utilised to deoxidise and desulfurise steel, as well as increase its hardness, toughness, and strength (Cairncross, Beukes, 2013; Wellbeloved et al., 1997). Whilst high-grade manganese ores can be product-tailored for ferroalloy production, lower-grade material, including tailings, may require feed preparation because smelting behaviour can be unpredictable, and will likely result in a reduced energy efficiency. Further, the loss of value through tailings and unutilised low-grade ore negates maximum resource utilisation efficiency. For material to be used as smelter feed in high-quality ferroalloy production, a manganese grade of at least 44 wt.% Mn and a Mn/Fe ratio of at least 7.5 is required after the blending of different ores and fluxes (Elliott, Barati, 2020). This paper focused on ferruginous manganese tailings obtained from the slimes dam at the Nchwaning mine in the Kalahari Manganese Field, however the results should be applicable to similar secondary materials. The material had an elevated and complex iron content that necessitates the selective removal of iron from the tailings for it to be used as smelter feed for ferroalloy production.

The selective removal of iron can be achieved using physical, hydrometallurgical, or pyrometallurgical beneficiation steps, or in combination. In most cases, physical processing steps alone are not sufficient to separate Fe from Mn (Singh et al., 2020). Hydrometallurgical methods show promise but pyrometallurgical beneficiation approaches have been chosen as the focus for this paper (Liu et al., 2019; Singh et al., 2020; You et al., 2017). Pyrometallurgical steps include the separation of the pre-reduction stage of smelting in the flowsheet that enables the upgrade of material and simultaneously reduces energy requirements (Larssen et al., 2020; Davies et al., 2023; Ernst et al., 2024; Schanche, Tangstad, 2021; Sarkar et al., 2024). Magnetic separation can be combined with pre-reductive roasting in flowsheet development to upgrade the material by selectively removing iron-rich phases that have a higher magnetic susceptibility, such as metallic iron or magnetite, from the manganese-rich phases, such as manganosite, following pre-reduction (Matabadal, 2022; Kivinen et al., 2010; Mpho et al., 2013).

Upgrading of ferruginous manganese tailings by hydrogen-rich reduction

Studies on Nchwaning ore have provided insights into the behaviour of this material during reduction in a CO-CO_2 environment. Previous research on the ferruginous Nchwaning ore has shown little success in upgrading the Mn/Fe ratio (Matabadal, 2022), underlining the need for further work towards this end. The primary reason the process did not achieve the desired Mn/Fe ratio was the formation of a FeO-MnO solid solution oxide phase that was difficult to reduce further and hindered magnetic separation of Fe and Mn (Matabadal, 2022). The formation of this composite oxide in ferruginous Mn ore has also been reported in other research studies under CO-CO_2 atmosphere conditions (El-Geassy et al., 2008; Zhang et al., 2017; Gao et al., 2019; Liu et al., 2019; Larssen et al., 2020; Davies et al., 2023). Pre-reduction roasting in the traditional CO-CO_2 atmosphere is therefore unlikely to yield the desired results. The use of hydrogen in the atmosphere has been shown to enhance both the extent and rate of reduction, resulting in the formation of metallic Fe, which is more readily separable in magnetic separation (Ernst et al., 2024). Furthermore, the addition of lime and/or silica flux to the unreduced ore has yielded mixed results in reducing iron and manganese oxides. Some studies have shown that the addition of CaO promoted Fe whisker formation (Zhong et al., 2017; Şeşen, 2001; Zhao et al., 2013), while others suggested that the formation of porous Fe layers increased the rate of reduction (Prakash et al., 2000; Shigematsu, Iwai, 1993; Ostrovski et al., 2004). Further, the investigation by Turkdogan and Vinters (1973) found that the addition of CaO retarded reduction, while the addition of SiO_2 had a negligible effect. Shigematsu and Iwai (1993) also found that the addition of SiO_2 can increase the rate of reduction of FeO to Fe. Interaction effects between the additives and original minerals will be limited as no liquid is formed at the considered reduction temperatures, but the additives can still influence reduction through solid state diffusion and ion diffusion (Zhao et al., 2013).

This paper investigated the pre-reduction of ferruginous manganese tailings from the Nchwaning mine in a hydrogen-rich atmosphere, followed by magnetic separation as a beneficiation process to produce ferroalloy smelter feed, aiming to support flowsheet development. To be suitable for ferroalloy smelter feed, the target specifications were an Mn grade of at least 44 wt.% and an Mn/Fe ratio of at least 7.5, while maximising Mn recovery.

Materials and methods

This paper conducted a thorough experimental design that investigated the influence of four key process variables: reduction temperature, degree of hydrogen enrichment, the addition of CaO, and the addition of SiO_2. The experimental approach is summarised in Figure 1. All drying was conducted at 110 °C for twelve hours to remove any surface moisture. The material was split into representative 30 g samples using a rotary splitter. The dried material had a D_{50} of 185 µm. The fine particle size required briquetting before being reduced, where polyvinyl alcohol was used as a binder. All magnetic separation was performed using a Davis tube, a wet magnetic separator, at a single, controlled magnetic intensity with 0.6A being fed to the electromagnet.

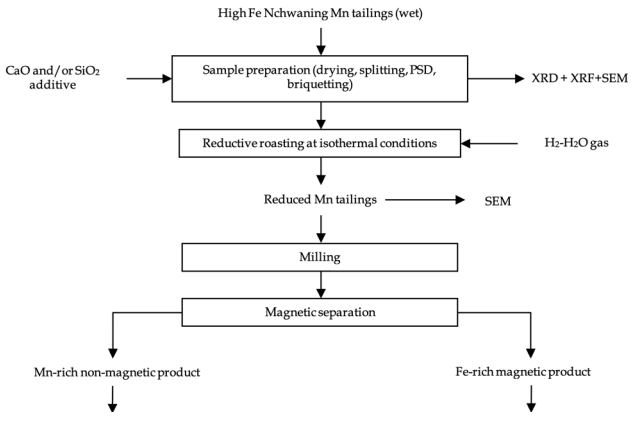

Figure 1—Summary of experimental approach and material flow

A controlled atmosphere retort furnace made of Kanthal APMT was used for all experimental runs. The schematic of the setup is shown in Figure 2. Gasses were fed to the controlled atmosphere furnace at the bottom, which allowed for them to be heated to the required temperature before entering. The retort was lowered into a chamber furnace during use. The gas flow was controlled using multiple gas flow controllers (MFC), and the water vapour was added to the inlet gas using a bubbler in a temperature-controlled water bath to entrain the vapour in the bubbled gas. Heating and cooling of the furnace was carried out in a nitrogen atmosphere. Hydrogen gas was introduced at a constant flow rate 2 NL/min, with a reduction time of two hours.

A central composite design was employed in this investigation; to represent curvature in response behaviour and to quantify the influence of interactions between process variables (Montgomery, 2013). The process conditions for the reduction temperature and the degree of hydrogen enrichment were selected using the iron oxide stability diagram in Figure 3. Manganese readily reduces to MnO before the reduction of iron oxides so the manganese oxide stability diagram is not necessary (Larssen et al., 2020). The reduction conditions, shown in red in Figure 3, were chosen to be well within

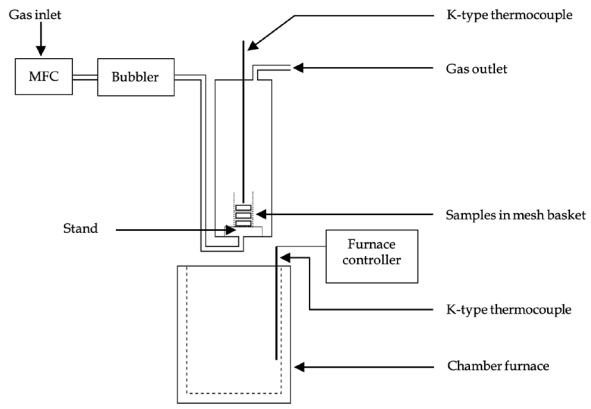

Figure 2—Controlled atmosphere furnace schematic

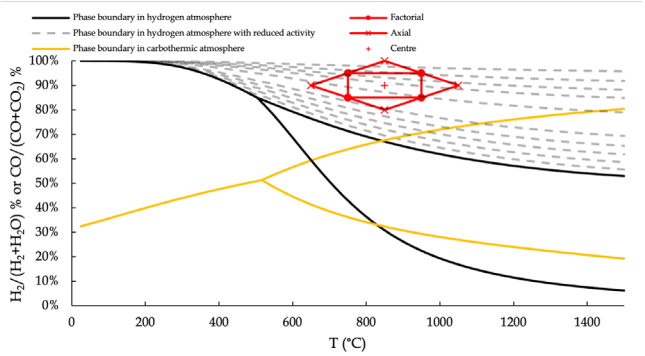

Figure 3—Iron oxide stability diagram in both carbothermic and hydrogen-enriched atmospheres with variable FeO activity. Experimental conditions investigated are marked in red, and the activity of FeO is indicated on each respective dashed line. Data obtained from FactSage (Bale et al., 2002)

Table 1
Summary of process conditions

Variable	High level	Low level	Centre point	High axial point	Low axial point
Temperature (°C)	950	750	850	1050	650
H2/(H2+H2O) (%)	95	85	90	100	80
CaO addition (wt.%)	6	2	4	8	0
SiO2 addition (wt.%)	6	2	4	8	0

Table 2
Chemical composition (wt.%) of untreated Nchwaning material according to X-ray fluorescence

	Mn	Fe	Ca	Si	Mg	Al	Na	P	Ti	L.O.I
Wt.%	44.52	17.42	3.39	1.67	0.26	0.10	0.04	0.02	0.02	2.86

Table 3
Mineral distribution of major Mn minerals in untreated Nchwaning material according to SEM-EDS analysis

Mineral	Bixbyite	Braunite	Braunite II	Manganite
Formula	$(Mn, Fe)2O_3$	$3(Mn, Fe)2O_3{\cdot}MnSiO_3$	$7(Mn, Fe)_2O_3{\cdot}CaSiO_3$	Ɣ-MnOOH
Wt.% of Mn minerals	26.5	15.2	54.5	3.8

the metallic Fe stability region, to promote the formation of metallic Fe, even when the activity of FeO is reduced. The dosage levels for CaO and SiO_2 were determined using the studies by Zhao et al. (2013) and Shigematsu and Iwai (1993) as guidelines. The levels used for each response variable are summarised in Table 1.

Results and discussion

Characterisation

The chemical composition of the untreated samples is presented in Table 2, with the Central Analytical Facility at Stellenbosch University conducting the X-ray fluorescence analysis. The material had an acceptable Mn grade of 44.5 wt.%, but was penalised by an elevated Fe content, which results in a low Mn/Fe ratio of 2.56.

X-ray diffraction was conducted by XRD Analytical and Consulting in Pretoria. The analysis revealed that the Nchwaning material contained five types of manganese minerals, making up 70.5 wt.% of the sample. Important minerals included braunite (61.2 wt.%), manganite (8.0 wt.%), hematite (23.2 wt.%), and calcite (6.1 wt.%). Only braunite and manganite made up more than one wt.% of the sample among the Mn minerals, and the analysis was unable to differentiate between braunite, braunite II, and bixbyite, as Cu k*a* radiation was used. To accurately account for the different Mn minerals, a bulk SEM-EDS analysis of the untreated material was conducted. The analysis normalised the number of cations for each candidate mineral, then used a charge balance to match each mineral grain to the most probable phase, according to the method proposed by Schumacher (1991). The distribution of the major Mn minerals present in the sample is presented in Table 3, with braunite II being the most abundant phase.

The Mn grade and the Fe content in the sample was highly variable from grain to grain, resulting in high variability in the Mn/Fe ratio as well. The distribution in Mn/Fe ratio for the major manganese minerals is illustrated in Figure 4, with braunite II exhibiting the lowest Mn/Fe ratio. The target Mn/Fe ratio to be suitable for ferroalloy production is 7.5, indicated by the dashed red line in Figure 4. The proportion of grains with a Mn/Fe ratio of less than 7.5 was 7%, 50%, and 76% for bixbyite, braunite, and braunite II, respectively, with 64% of the total Mn grains falling below this.

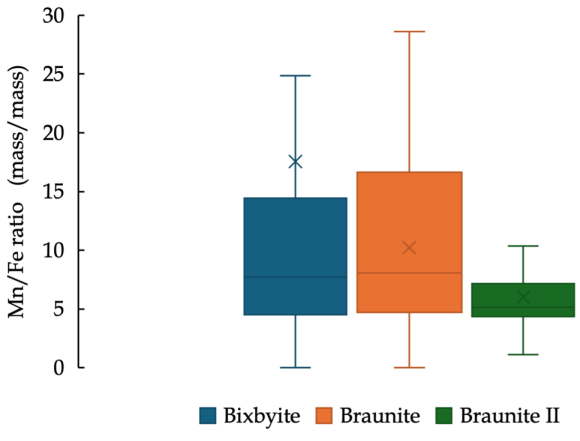

Figure 4—Box and whisker plot showing Mn/Fe ratio in manganese minerals

Therefore, braunite II posed the most significant challenge in upgrading the Mn/Fe ratio.

The manganese minerals also contained a high degree of iron present in solution, with up to 39 wt.% of the total iron in the sample being found in these Mn minerals. The Mn mineral grains were found to contain up to 20.4 wt.% Fe, with braunite II having a mean Fe content of 12.3 wt.%. These high concentrations of Fe in manganese minerals fall within expected theoretical limits, with work by Momoi et al. (1985) finding up to 40 wt.% Fe in synthesised ferrian braunite. The high iron content complicated separation as the highest possible Mn/Fe ratio achievable was 6.33, if all hematite present was removed, without removing the iron in the Mn minerals. Therefore, to achieve an Mn/Fe ratio of 7.5, Fe had to be separated from the Mn minerals as well, or the most ferruginous Mn grains had to be removed.

Experimental results

The results of the XRF analysis of the treated magnetic and non-magnetic fractions were used to calculate the Mn/Fe ratio, Mn grade, and Mn recovery to the non-magnetic stream. The highest Mn/Fe ratio achieved was 4.52 for an experimental run where all operating conditions were at their low level (Table 1). This test run also resulted in an Mn grade of 57.4 wt.% and an 85.5% recovery of Mn.

Following reduction, the metallic iron that formed was found to have distinctly different sized globules, depending on mineral that the iron was initially associated with. The size analysis was performed using Fiji image processing software. The metallic iron that formed from the reduction of hematite resulted in larger particles with a feret diameter from 50 µm to 600 µm, while the metallic iron globules that formed from the iron in solid solution in manganese minerals resulted in small particles with a feret diameter between 0.1 µm to 2 µm. The particle size distribution (PSD) after milling influences the liberation of the metallic iron, and therefore the subsequent separation efficiency. The iron particles are more likely to be well liberated if the particle size is fine, however, this would result in higher milling costs and increase the difficulty of solids handlings. The D_{80} passing size for the milled material was 80.6 µm, which makes it unlikely that the small iron globules would be well liberated.

Statistical modelling

Statistical analysis, using Statistica, was used to isolate the influence of each factor on the response variables. Second-order models were regressed for each response using response surface methodology. The models yielded adjusted R^2 values of 0.77, 0.81, and 0.83 for the Mn/Fe ratio, Mn grade, and Mn recovery to the non-magnetic stream, respectively. Pareto charts were used to select statistically significant factors for further analysis.

Changes in the reduction temperature and degree of hydrogen enrichment had similar influences on all response variables, as they both determine the reduction conditions present. However, the reduction temperature had a more significant influence on the response variables than the degree of hydrogen enrichment. As the temperature increased, the amount of mass reporting to the magnetic stream initially increased sharply before plateauing at higher temperatures as reduction reached completion (Figure 5). This is due to the reduction from wustite (FeO) to metallic Fe being the last to occur, thus increasing the magnetic susceptibility of the treated sample. The addition of silica had a positive interaction effect with the reduction temperature on the mass pull, where the influence of SiO2 addition is negligible at low temperatures but markedly increases the mass pull at temperatures greater than 850 °C.

The predicted influence of each the lime and silica additions on the Mn grade of the non-magnetic stream is presented in Figure 6. The error bars represent the 95% confidence interval for the model. Both additives had a negative impact on the Mn grade, due to diluting the overall stream. The addition of CaO was not found to have a significant influence on any other response variable. Therefore, CaO did not influence the reduction process, which is supported by the perfectly linear negative relationship between lime addition and Mn grade. On the other hand, the addition of SiO_2 also dilutes the stream initially, but the Mn grade plateaus at higher addition levels due to the interaction effect between the reduction temperature and silica addition.

The predicted influence of each reduction temperature and the silica additions on the Mn/Fe ratio is presented in Figure 7. The Mn/Fe ratio decreased sharply with the initial increase in reduction temperature, then plateaued at higher temperatures as the full extent of reduction was reached. The higher reduction temperature caused more Fe globules to form in Mn grains, which were not adequately liberated during milling, resulting in excess Mn being carried to the magnetic stream – therefore lowering the Mn/Fe ratio in the non-magnetic stream as the reduction temperature increased. The addition of silica initially lowered the Mn/Fe ratio, before reaching a minimum Mn/Fe at about 4 wt.% SiO_2 added and increased thereafter due to the interaction between SiO_2 and the reduction temperature.

Mineral texture analysis

A detailed mineral texture analysis of the treated samples was conducted to better understand the behaviour seen in the statistical models. This analysis was performed using SEM-EDS and optical microscopy in combination. All textural analysis is performed on the treated samples before milling and magnetic separation.

At the lowest temperature, that is, 650°C, not all the treated hematite grains were fully reduced, thus limiting the degree of separability due to a difference in magnetic susceptibility. No iron globules were found to form in the Mn mineral grains. When the reduction temperature reached 750 °C, all treated

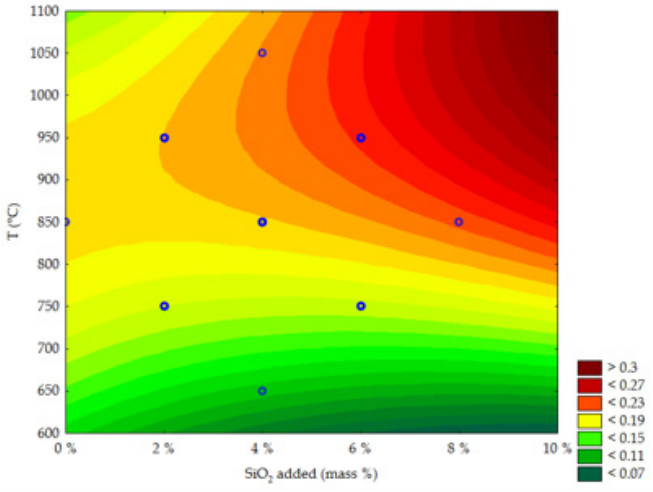

Figure 5—Response contour showing the predicted mass pull to the magnetic stream with respect to both the mass of silica added and the reduction temperature when both other factors are at their centre point level (H2 = 90% and CaO added = 4 wt.%)

hematite was fully reduced (Figure 8), with only small regions in the middle of metallic Fe globules within treated hematite exhibiting incomplete reduction. These mostly reduced Fe globules in Figure 8, which illustrates how the reduction proceeds from the outside of the globule towards the centre due to mass transfer limitations as the dense metallic iron layer forms , as well as the porous nature of the grain. These large pure metallic Fe grains should have been well liberated and reported to the magnetic stream during magnetic separation.

The treated manganese mineral grain, illustrated in Figure 9, has

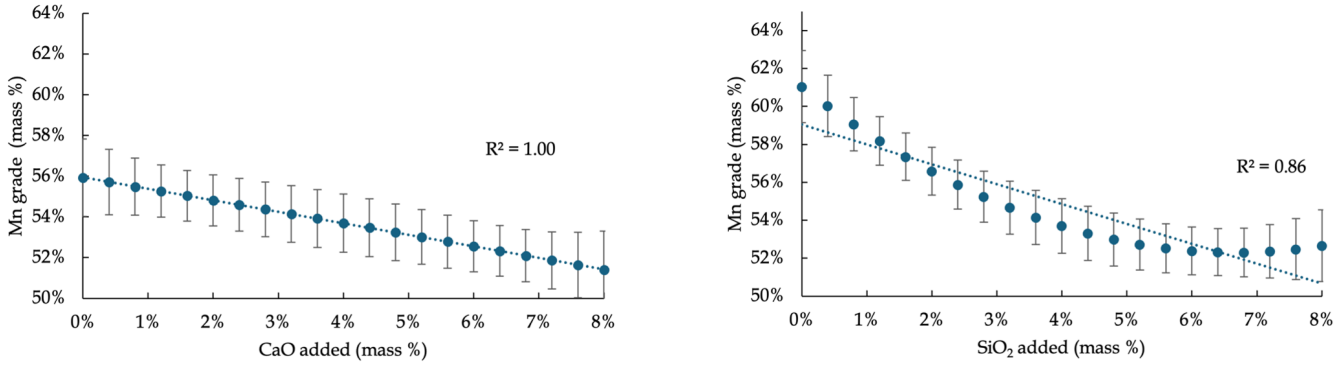

Figure 6—Curves showing the predicted change in manganese grade in the non-magnetic stream with respect to (a) the mass of lime added, and (b) the mass of silica added when all other factors are at their centre point level (T = 850°C, H_2 = 90%, CaO added = 4 *w*t.%, and SiO_2 added = 4 *w*t.%)

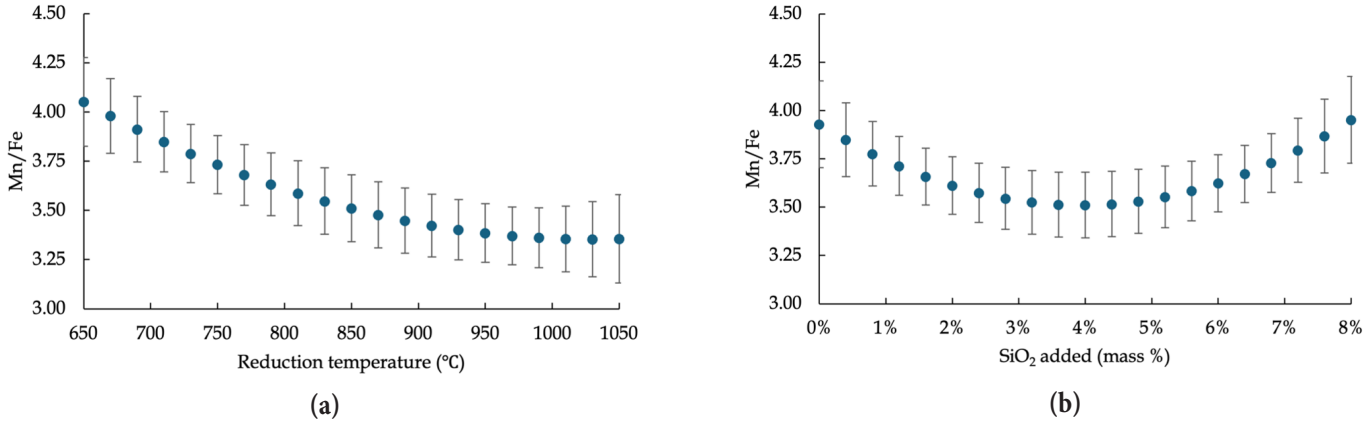

Figure 7—Curves showing the predicted change in Mn/Fe in the non-magnetic stream with respect to (a) the reduction temperature, and (b) the mass of silica added when all other factors are at their centre point level (T = 850°C, H_2 = 90%, CaO added = 4 wt.%, and SiO_2 added = 4 wt.%)

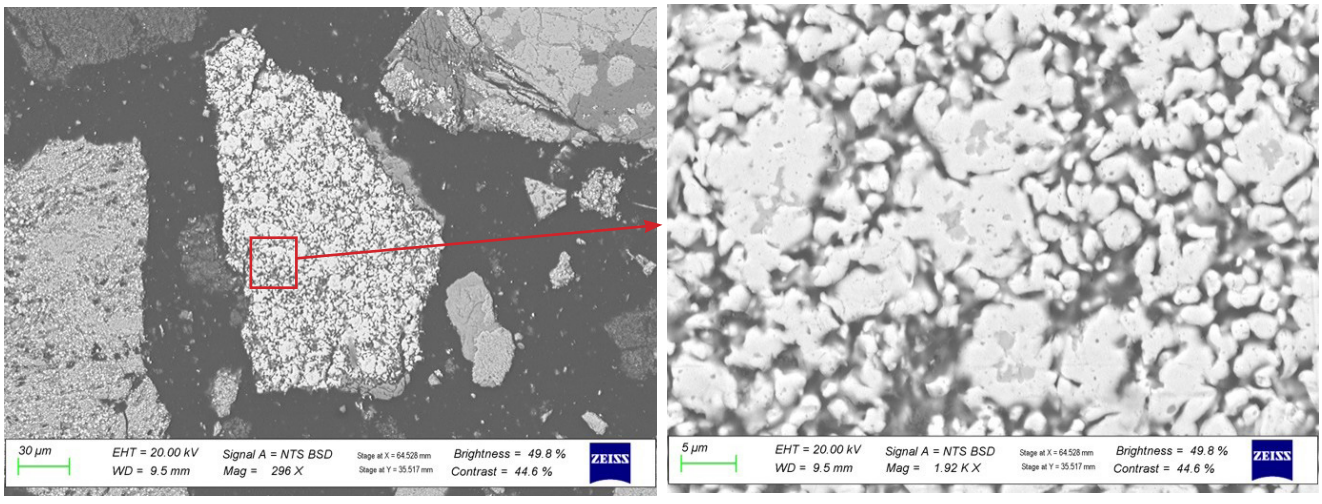

Figure 8—SEM images illustrating treated hematite at (a) 296x, and (b) 1920x. Sample treated at 750 °C; 85% H_2; 2 wt.% CaO added; 6 wt.% SiO_2 added

been reduced to form a stable solution of manganosite containing wustite and other minor impurities. This grain contained 13.1 wt.% iron, the highest iron content found in this experimental run without any Fe-alloy globules forming. The median Fe content for braunite II was 11.8 wt.%, and the overall median Fe content for Mn minerals was 10.5 wt.% for the Nchwaning material. Therefore, most Mn mineral grains did not have a high enough Fe content for Fe-alloy globules to form. Without the formation of any Fe-alloy globules to increase the magnetic susceptibility, these grains should have correctly reported to the non-magnetic stream. The grains illustrated in Figure 9 and Figure 10 are from the best performing experimental run.

The treated manganese mineral grain (Figure 10) had a higher Fe content (20.3 wt.% Fe) than the grain in Figure 9. The higher Fe content resulted in Fe-alloy globules forming with a median Feret diameter of 0.74 µm. These globules contained 70.0 wt.% Fe and 23 wt.% Mn. The globules would have increased the magnetic susceptibility of their associated particle after milling and will likely have reported to the magnetic stream, along with any entrained Mn, lowering the Mn/Fe of the non-magnetic stream.

The trend where a higher Fe content in Mn mineral grains resulted in Fe-alloy globules forming, was evident in all test runs. Additionally, a lower iron content was required for globules to form in stronger reducing conditions. These observations are summarised in Table 4, with Fe-alloy globules forming in grains with lower Fe content in relatively stronger reducing conditions (850 °C and at least 90% H2). This behaviour was due to the relationship between the activity of a phase and its concentration (Ganguly, 2001).
In stronger reducing conditions, the threshold to form Fe-alloy globules was lower, and these globules therefore formed in more Mn mineral grains. Thus, raising their magnetic susceptibility and causing more entrained Mn to incorrectly report to the magnetic stream, which resulted in a decreased Mn/Fe ratio in the non-magnetic stream at stronger reducing conditions. This behaviour could be used, in conjunction with variable magnetic intensity of the magnetic separator, to target Mn grains with the highest Fe and separate on a grain by grain basis, rather than only the Fe-alloy globules.
In experimental runs with both an elevated temperature (> 850 °C)

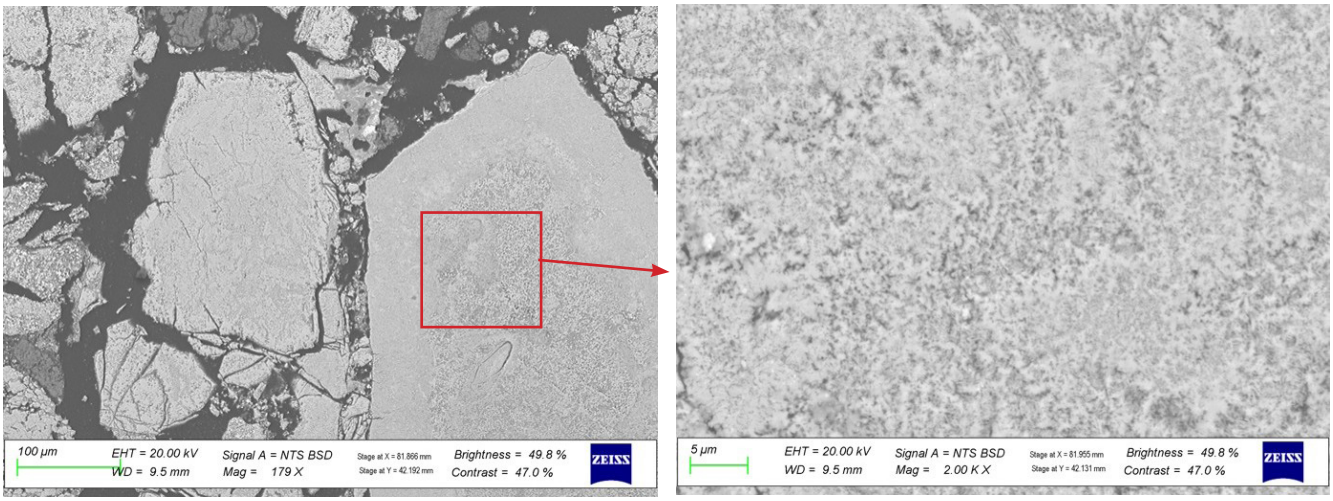

(a) (b)

Figure 9—SEM images illustrating a treated manganese mineral grain with no Fe-alloy flecks at (a) 179x, and (b) 2000x. Sample treated at 750 °C; 85% H_2; 2 *w*t.% CaO added; 2 *w*t.% SiO_2 added

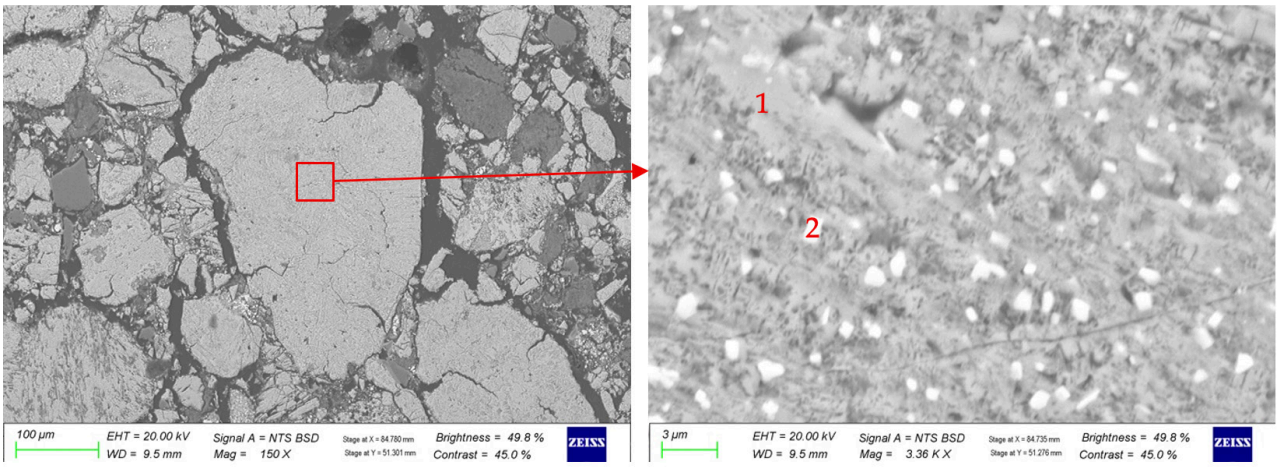

(a) (b)

Figure 10—SEM images illustrating a treated manganese mineral grain with Fe-alloy flecks at (a) 150x, and (b) 3360x. The labels in (b) refer to (1) Mn oxide and (2) Fe alloy. Sample treated at 750°C; 85% H_2; 2 wt.% CaO added; 2 wt.% SiO_2 added

and silica additions (> 4 wt.% added), a new structure was found in treated manganese mineral grains with an elevated Si and Ca level, likely braunite II, illustrated in Figure 11. Most Mn mineral grains contained just the manganese-rich oxide phase and Fe-alloy globules, if they formed. This new structure also contained an Mn-Ca silicate phase that contains 21 wt.% Mn, 20 wt.% Ca, 14 wt.% Si, and 5 wt.% Fe – whereas the Mn oxide phase contained 74 wt.% Mn, 3 wt.% Fe, 3 wt.% Ca, and 2 wt.% Si. The most important difference, due to its ramifications on the magnetic separability of Mn, is the formation of large, thin Fe-alloy globules that were not likely to have been liberated well during milling. Therefore, the formation of this new structure in treated braunite II grains resulted in an increased mass pull to the magnetic stream and a decreased Mn/Fe ratio in the non-magnetic stream. This behaviour accounts for the interaction effect between the reduction temperature and silica additions that was discussed during the statistical analysis, although it is unclear what mechanism could be causing it. It is noted that the doped silica is not likely to have transported into the grain, as no liquid phases should have formed during reduction at the experimental conditions investigated. Therefore, the elevated Ca and Si in the Mn-Ca silicate phase likely originate from the original braunite II grain, and are merely more concentrated in this new phase.

Suppose perfect liberation of all metallic Fe, formed from the

Table 4

Comparison of Fe contents in Mn mineral grains required for Fe-alloy globules to begin forming

T (°C)	H_2 (%)	Highest Fe bulk without globules (wt.%)	Lowest Fe bulk with globules (wt.%)
750	85	13.1	13.6
750	85	8.6	16.8
650	90	21.0	62.2
850	80	5.3	11.0
850	100	4.0	7.4
850	90	5.4	7.7

Table 5

Comparison of theoretical maximum Mn/Fe achievable and actual performance from experimental runs

T (°C)	H_2 (%)	CaO added (wt.%)	SiO_2 added (wt.%)	Average Mn/Fe initial	Average Mn/Fe oxide	Mn/Fe achieved in non-magnetic stream	Per cent achieved
750	85	2	2	3.75	5.47	4.52	67.3
750	85	6	2	4.08	5.11	4.22	65.3
850	100	4	4	5.11	9.42	3.55	14.6
950	95	6	6	N/A	20.20	3.58	5.8
850	90	4	4	7.24	10.23	3.53	12.8

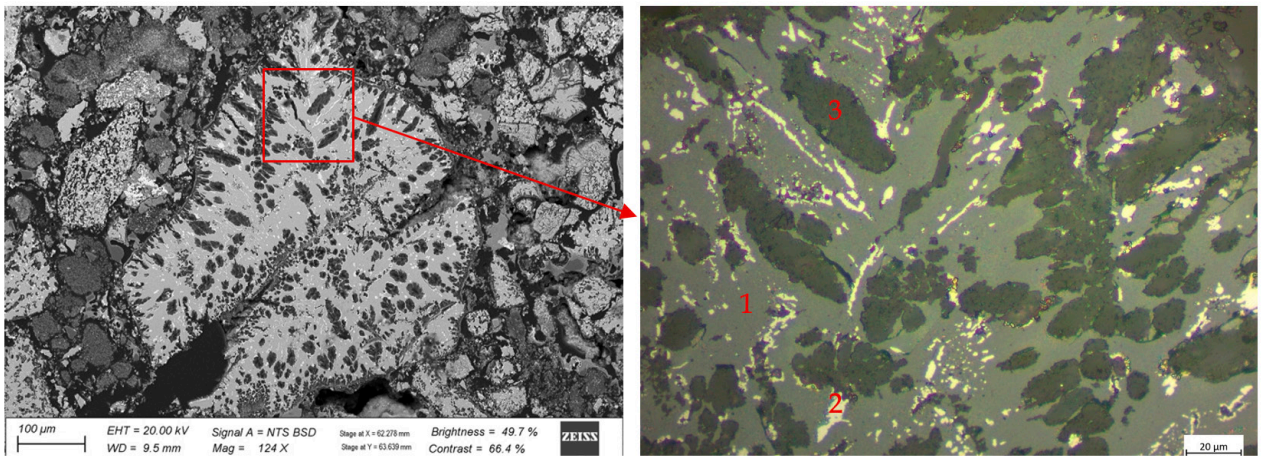

(a) (b)

Figure 11—Images illustrating a treated manganese mineral grain taken using (a) SEM, and (b) an optical microscope. The labels in (b) refer to (1) Mn oxide, (2) Fe alloy, and (3) Mn-Ca silicate. Sample treated at 950°C; 95% H2; 6 wt.% CaO added; 6 wt.% SiO2 added

reduction of both hematite and Fe-alloy globules in Mn minerals, and then the perfect subsequent magnetic separation were possible. In that case, the theoretical maximum Mn/Fe ratio that can be achieved was the Mn/Fe ratio in the oxide. Iron that remained trapped in solution with the Mn oxide will not be separated. To understand how well the magnetic separation worked, the actual upgrade in Mn/Fe (from the initial ratio of 2.56) can be compared to the theoretical upgrade possible (Table 5). The experimental runs with relatively milder reducing conditions (750 °C and 85% H_2) had a lower theoretical maximum Mn/Fe ratio, due to much of the iron remaining in solid solution, but they achieved more than 65% of this maximum. Conversely, the runs with relatively stronger reducing conditions had a much higher theoretical maximum Mn/Fe due to the formation of Fe-alloy globules, but these same globules cause entrained manganese to report to the incorrect stream, and less than 15% of this maximum is achieved. The alloy globules that form with the Mn minerals are too small to be well liberated after milling.

Conclusions

The hydrogen-rich reductive roast followed by magnetic separation process was investigated for its suitability in upgrading ferruginous manganese tailings from the Nchwaning mine tailings dam. The goal of the process was to upgrade the material to be suitable for ferroalloy production, which requires a manganese grade of 44 wt.% and an Mn/Fe ratio of at least 7.5.

The results of the optimisation study indicate that the target Mn/Fe ratio was not achievable within the investigated range of process conditions. The best conditions achieved an Mn/Fe ratio of 4.52, an Mn grade of 57.4 wt%, and a manganese recovery of 85.5 wt. at 750 °C, 2 wt.% CaO added, 2 wt.% SiO_2 added, and in 85% H_2. While the Mn/Fe ratio is below the desired 7.5, the high Mn grade of 57.4 wt.% means that the product can be blended with low-grade carbonate ores with a low Fe content to produce higher quality ferroalloy smelter feed.

The mineralogical variability had a significant influence on the reductive roasting and subsequent magnetic separation. The variable Fe content in Mn grains was found to determine whether Fe-alloy globules were likely to from under specific reducing conditions. The stronger the reducing conditions, the lower the threshold Fe content required to form Fe-alloy globules. At reduction temperatures of 950 °C or higher (and with elevated silica), the treated braunite II grains were found to form a new Mn-Ca silicate phase that allowed for the formation of larger Fe-alloy globules. However, the PSD of the phases after milling, and the intensity of the magnetic separator did not allow for these Fe globules to be well liberated and subsequently separated.

The statistical analysis revealed that relatively weaker reducing conditions resulted in the best Mn/Fe ratio, Mn grade, and Mn recovery. This behaviour was due to the reducing conditions being still strong enough to entirely reduce the discrete hematite particles into metallic Fe without reducing much of the Fe within the solid solution in Mn grains. The metallic Fe was well liberated and therefore efficiently separated. Stronger reducing conditions led to the formation of magnetic Fe-alloy globules in Mn grains, which were poorly liberated after milling, causing some of these globules to report to the magnetic stream along with associated Mn. The loss of Mn to the magnetic stream resulted in a decreased Mn/Fe ratio, Mn grade, and Mn recovery.

Recommendations

The biggest obstacle to the separation of Mn and Fe was the degree of liberation of the iron alloy globules that formed in the manganese grains. The size of the Fe globules formed was too small to feasibly liberate via conventional milling. It is therefore recommended to investigate a narrower temperature range with more experimental levels that focuses on only generating Fe globules in high Fe manganese minerals, then separate these larger particles rather than focusing on those less than 2 µm in diameter. The strength of the magnetic field can also be added as a parameter to better separate the Fe particles.

Silica additions had a significant influence on the reduction and subsequent magnetic separation, but no conclusive evidence was found regarding the exact mechanism by which this was achieved. It is therefore recommended to conduct further tests that focus on this, and utilise extensive mineral characterisation, such as QEMSCAN, to better understand the mechanisms at play.

References

Bale, C.W., Chartrand, P., Degterov, S.A., Eriksson, G., Hack, K., Mahfoud, R.B., Melancon, J., Pelton, A.D., Petersen, S. 2002. FactSage Thermochemical Software and Databases. Calphad, vol. 26, pp. 189–228.

Cairncross, B., Beukes, N.J. 2013. The Kalahari Manganese Field: The Adventure Continues, Struik Nature.

Davies, J., Tangstad, M., Schanche, T.L., Du Preez, S.P. 2023. Pre-reduction of United Manganese of Kalahari Ore in CO/CO2, H2/H2O, and H2 Atmospheres. *Metallurgical and Materials Transactions B*, vol. 54, pp. 515–535.

El-Geassy, A.A., Nasr, M.I., Omar, A.A., Mousa, E.A. 2008. Isothermal reduction behaviour of MnO2doped Fe2O3compacts with H2at 1073–1373 K. *Ironmaking & Steelmaking*, vol. 35, pp. 531–538.

Elliott, R., Barati, M. 2020. A review of the beneficiation of low-grade manganese ores by magnetic separation. *Canadian Metallurgical Quarterly*, vol. 59, pp. 1–16.

Ernst, M.S., Tangstad, M., Du Preez, S.P. 2024. Pre-reduction of Nchwaning manganese ore in CO/CO2, H2/H2O, and H2 atmospheres. *Minerals Engineering*, vol. 216.

Ganguly, J. 2001. Thermodynamic modelling of solid solutions. *EMU Notes in Mineralogy.*

Gao, L., Liu, Z., Pan, Y., Feng, C., Chu, M., Tang, J. 2019. Systematic study on separation of Mn and Fe from ferruginous manganese ores by carbothermic reduction roasting process: Phase transformation and morphologies. *Journal of Materials Research and Technology*, vol. 8, pp. 5591–5609.

Kivinen, V., Krogerus, H., Daatvittila, J. 2010. Upgrading of Mn/Fe Ratio of Low-Grade Manganese Ore for Ferromanganese Production. *The Twelth International Ferroalloys Congress, 2010 Helsinki.*

Larssen, T.A., Senk, D., Tangstad, M. 2020. Reduction of Manganese Ores in CO-CO2 Atmospheres. *Metallurgical and Materials Transactions B*, vol. 52, pp. 363–381.

Liu, B., Zhang, Y., Lu, M., Su, Z., Li, G., Jiang, T. 2019. Extraction and separation of manganese and iron from ferruginous

manganese ores: A review. *Minerals Engineering*, vol 131, pp. 286–303.

Matabadal, Y. 2022. Evaluation of the Reduction Roast-Magnetic Separation Process to Upgrade Low-Grade Ferruginous Manganese Ore Fines. MEng, *University of Pretoria*.

Momoi, H., Horikawa, M., Fujino, K. 1985. Synthesis and characterisation of ferrian braunite. *Mineralogical Journal*, vol. pp. 12, 367–375.

Montgomery, D.C. 2013. Design and Analysis of Experiments. 8th ed.: John Wiley & Sons.

Mpho, M., Samson, B., Ayo, A. 2013. Evaluation of reduction roasting and magnetic separation for upgrading Mn/Fe ratio of fine ferromanganese. *International Journal of Mining Science and Technology*, vol. 23, pp. 537–541.

Ostrovski, O., Anacleto, N., Ganguly, S. 2004. Reduction of manganese ores by methane-containing gas. Tenth International Ferroalloys Congress, 2004 Cape Town, South Africa.

Prakash, S., Goswami, M.C., Mahapatra, K.S., Ghosh, K.C., Das, S.K., Sinha, A. N., Mishra, K.K. 2000. Morphology and reduction kinetics of fluxed iron ore pellets. *Ironmaking & Steelmaking*, vol. 27.

Sarkar, A., Schanche, T.L., Wallin, M., Safarian, J. 2024. Evaluating the Reaction Kinetics on the H2 Reduction of a Manganese Ore at Elevated Temperatures. *Journal of Sustainable Metallurgy,* vol. 10, pp. 2085–2103.

Schanche, T.L., Tangstad, M. 2021. Prereduction of Nchwaning Ore in CO/CO2/H2 Gas *Mixtures. Minerals*, vol. 11.

Schumacher, J.C. 1991. Empirical ferric iron corrections: necessity, assumptions, and effects on selected geothermobarometers. *Mineralogical Magazine*, vol. 55, pp. 3–18.

Şeşen, M.K. 2001. The influence of CaO on the precipitation behaviour of iron in the reduction of iron oxide. *Scandinavian Journal of Metallurgy*, vol. 30, pp. 1–7.

Shigematsu, N., Iwai, H. 1993. Effect of the Addition of SiO_2 and SiO_2–CaO on the Reduction of Dense Wüstite at High Temperatures. Tetsu-to-Hagane *(Journal of the Iron and Steel Institute of Japan)*, vol. 79, pp. 913–920.

Singh, V., Chakraborty, T., Tripathy, S.K. 2020. A Review of Low Grade Manganese Ore Upgradation Processes. *Mineral Processing and Extractive Metallurgy Review*, vol. 41, pp. 417–438.

Turkdogan, E.T., Vinters, J. V. 1973. Reducibility of iron ore pellets and effect of additions. *Canadian Metallurgical Quarterly*, vol. 12, pp. 9–21.

Wellbeloved, D.B., Craven, P.M., Waudby, J.W. 1997. Manganese and manganese alloys. In: ELVERS, B., HAWKINS, S., SCHULZ, G. (eds.) Ullman's Encyclopedia of Industrial Chemistry. New York: John Wiley & Sons.

You, Z., Li, G., Peng, Z., Zhang, Y., Qin, L., Jiang, T. 2017. Reductive roasting of iron-rich manganese oxide ore with elemental sulfur for selective manganese extraction. *Journal of Mining and Metallurgy, Section B: Metallurgy*, vol. 53, pp. 115–122.

Zhang, Y., Du, M., Liu, B., Su, Z., Li, G., Jiang, T. 2017. Separation and recovery of iron and manganese from high-iron manganese oxide ores by reduction roasting and magnetic separation technique. *Separation Science and Technology*, vol. 52, pp. 1321–1332.

Zhao, Z.L., Tang, H.Q., Guo, Z.C. 2013. Effects of CaO on precipitation morphology of metallic iron in reduction of iron oxides under CO atmosphere. *Journal of Iron and Steel Research International*, 20, 16–24.

Zhong, H., ER, D., Wen, L. 2017. Theoretical study on influence of CaO and MgO on the reduction of FeO by CO. *Applied Surface Science*, vol. 399, pp. 630–637. ◆

YPC EVENTS SERIES 2026

The role of youth and young professionals in Future Proofing African Mining, Today

BACKGROUND AROUND THE THEME

- Focus on sustainability and innovation
- Inclusivity and job creation
- Aligns to the Mining Indaba theme
- Beyond mining

THE EVENTS FOR THE MONTH:

YPC Student Debate presented by the SAIMM Johannesburg Branch: 27 August 2026, DRA Head Office, Sandton, Johannesburg.

Topic: Does mining provide additional value apart from only extracting resources within communities.

Debate Topics: Fostering innovation, infrastructure development and economic growth across various sectors.

The Johannesburg Branch in partnership with the Young Professionals Council is proud to present the Student Debate featuring The University of Johannesburg and University of the Witwatersrand.
This event will provide a stage for students from The University of Johannesburg and University of the Witwatersrand, within the minerals discipline to present compelling arguments on industry relevant themes.

Young Professionals Conference: 29-30 September 2026, Mintek, Randburg, Johannesburg

Topic: The role of youth and young professionals in Future Proofing African Mining, Today
The conference promises to be an engaging and informative event that will explore the latest trends, ideas, and innovations in the minerals industry. This conference offers young professionals the opportunity to network with peers and industry experts, establish professional relationships, and collaborate on future projects. A conference dedicated to young professionals emphasising the importance of empowering young professionals to lead the way in driving innovation and sustainability in the South African minerals industry.

Student Colloquium: 28 October 2026, Mintek, Randburg, Johannesburg.

Topic: Adapting the African Mining industry to changing global trends to ensure long term sustainability.

The Southern African Institute of Mining and Metallurgy has been organizing and presenting the annual Student Colloquium since 2002, to afford the best final-year mining and metallurgical students an opportunity to present their final year projects to an audience of mining and metallurgical industry experts.
Students are given an opportunity and platform to showcase their best research and innovation that contributes to advancing the mining and minerals industry to greater heights

FOR FURTHER INFORMATION CONTACT:
Gugu Charlie,
Conference and Events Coordinator
E-mail: gugu@saimm.co.za
Tel: +27 11 538-0238 Web: www.saimm.co.za